Electronic Supplementary Information (ESI)

Controlled growth of vertical 3D $MoS_{2(1-x)}Se_{2x}$ nanosheets for efficient and stable hydrogen evolution reaction

Xiaoshuang Chen,[ab] Zhiguo Wang,[c] Yunfeng Qiu,[a] Jia Zhang,[a] Guangbo Liu,[a] Wei Zheng,[a] Wei Feng,[a] Wenwu Cao,[b] PingAn Hu*[a]and Wenping Hu*[bd]

[a]Key Lab of Microsystem and Microstructure of Ministry of Education, Harbin Institute of Technology, Harbin 150080, China. E-mail: hupa@hit.edu.cn

[b]Department of Physics, Harbin Institute of Technology, Harbin 150080, China

[c]School of Physical Electronics, Center for Public Security Information and Equipment Integration Technology, University of Electronic Science and Technology of China, Chengdu, 610054, P.R. China

[d]Key Laboratory of Organic Solids, Institute of Chemistry, Chinese Academy of Sciences, Beijing 100190, China. E-mail: huwp@iccas.ac.cn

Simulation details and methods

All the calculations were performed by using density functional theory (DFT) calculations as implemented in the Vienna *ab initio* package (VASP).[S1] Spin-polarization was considered for all the simulations. The projector augmented wave (PAW) method [S2] was used to describe electron-ion interaction, while the generalized gradient approximation using the Perdew-Burke-Ernzerhof (PBE) functional was used to describe the electron exchange-correlation. A plane wave basis was set up to an energy cut off of 520 eV. A 6×6 supercell of $MoS_{2(1-x)}Se_{2x}$ monolayer was used to investigate the adsorption of hydrogen. A 25 Å vacuum space was constructed to avoid the periodical image interactions between two adjacent $MoS_{2(1-x)}Se_{2x}$ layers. The Brillouin zone was integrated using the Monkhorst-Pack scheme [S3] with 3×3×1 *k*-grid. All the atomic positions and cell parameters were relaxed using a conjugate gradient minimization until the force on each atom is less than 0.02 eV $Å^{-1}$.

Gibbs free-energy of the adsorption atomic hydrogen was calculated using equation (1):

$$\Delta G_H^0 = \Delta E_H + \Delta E_{ZPE} - T\Delta S_H \quad (1)$$

Where ΔE_{ZPE} and ΔS_H are the zero-point energy and entropy difference of hydrogen in the adsorbed state and the gas phase, respectively. The hydrogen adsorption energy ΔE_H for hydrogen in pritine $MoS_{2(1-x)}Se_{2x}$ is calculated with the following expression:

$$\Delta E_H = E_{MoS_{2(1-x)}Se_{2x}+H} - E_{MoS_{2(1-x)}Se_{2x}} - \frac{1}{2}E_{H_2} \quad (2)$$

where $E_{MoS_{2(1-x)}Se_{2x}+H}$ and $E_{MoS_{2(1-x)}Se_{2x}}$ are the total energies of $MoS_{2(1-x)}Se_{2x}$ with and without hydrogen adsorption, respectively. E_{H_2} is the energy of a gas phase hydrogen molecule.

The hydrogen adsorption energy ΔE_H for hydrogen adsorbed in $MoS_{2(1-x)}Se_{2x}$ with S and Se vacancies is calculated with the following expression:

$$\Delta E_H = E_{MoS_{2(1-x)}Se_{2x}(\mathrm{vac})+H} - E_{MoS_{2(1-x)}Se_{2x}(\mathrm{vac})} - \frac{1}{2}E_{H_2} \quad (3)$$

where $E_{MoS_{2(1-x)}Se_{2x}(\mathrm{vac})+H}$ and $E_{MoS_{2(1-x)}Se_{2x}(\mathrm{vac})}$ are the total energies of $MoS_{2(1-x)}Se_{2x}$ with vacancy and with and without hydrogen adsorption, respectively.

The calculated frequencies of H_2 gas is 4345 cm^{-1}, 58 cm^{-1}, and 42 cm^{-1}. The contribution from the configurational entropy in the adsorbed state is small and is neglected. So the entropy of hydrogen adsorption as $\Delta S_H = \frac{1}{2}S_{H_2}$ where S_{H_2} is the entropy of molecule hydrogen in the gas phase at standard conditions.[S4] With these values the Gibbs free energy of equation (1) can be rewritten as:

$$\Delta G_H^0 = \Delta E_H + 0.29 \quad (4)$$

The defect formation energy E_f of S/Se vacancy was calculated from the following expression:[S5]

$$E_f(\text{Vac}) = E(\text{Vac}) - E(\text{pristine}) + \mu_{\text{S/Se}} \quad (5)$$

where E(Vac) is the total energy of the supercell containing a relaxed S or Se vacancy, E(pristine) is the total energy of the same pristine supercell, $\mu_{\text{S/Se}}$ is the chemical potential of S or Se.

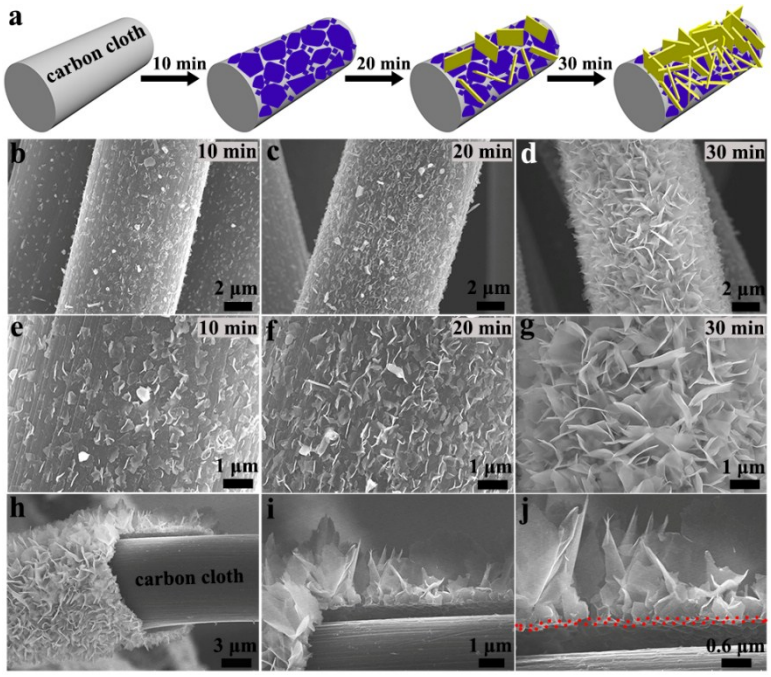

Fig. S1 (a) schematic diagram, (b-g) different magnification SEM images for growth process of vertically oriented 3D $MoS_{2(1-x)}Se_{2x}$ nanosheets on carbon cloth with different growth time (10, 20, 30 min), (h-j) different magnification side-view SEM images of vertically oriented 3D $MoS_{2(1-x)}Se_{2x}$ nanosheets on the damaged region at the growth time of 30 min.

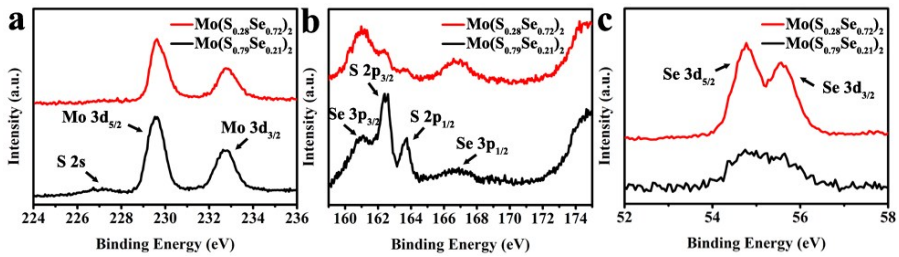

Fig. S2 XPS spectra of Mo 3d, S 2s, S 2p, Se 3p and Se 3d of vertically oriented 3D $Mo(S_{0.79}Se_{0.21})_2$ and $Mo(S_{0.28}Se_{0.72})_2$ alloy nanosheets.

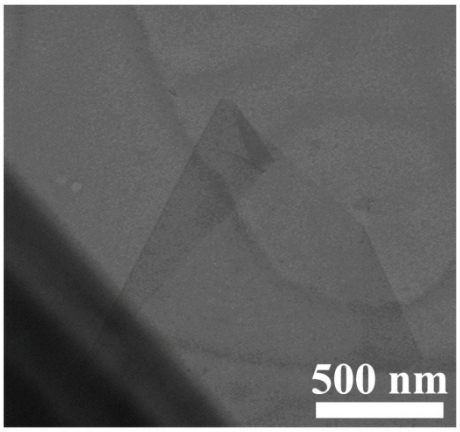

Fig. S3 Dark-field TEM image of vertically oriented 3D $Mo(S_{0.53}Se_{0.47})_2$ nanosheets.

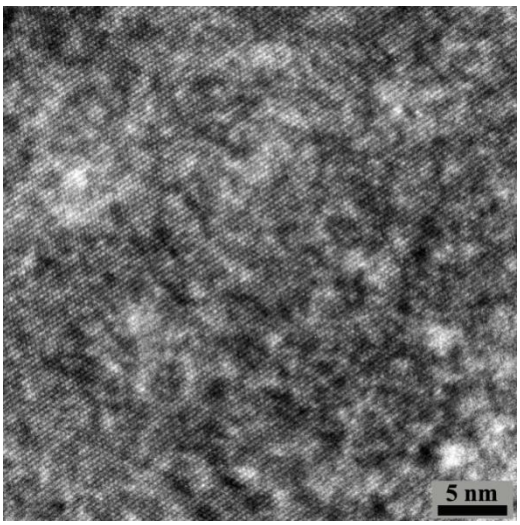

Fig. S4 Large region HRTEM image of vertically oriented 3D $Mo(S_{0.53}Se_{0.47})_2$ nanosheets.

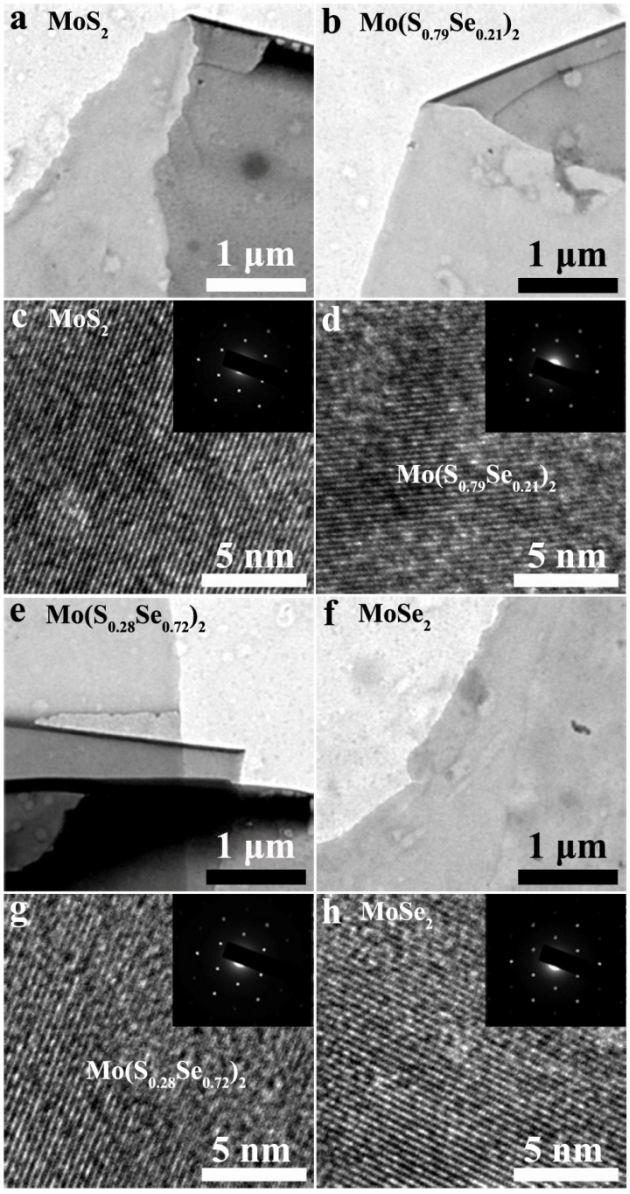

Fig. S5 TEM, HRTEM images and SAED patterns of vertically oriented 3D (a,c) MoS_2, (b,d) $Mo(S_{0.79}Se_{0.21})_2$, (e,g) $Mo(S_{0.28}Se_{0.72})_2$ and (f,h) $MoSe_2$ nanosheets.

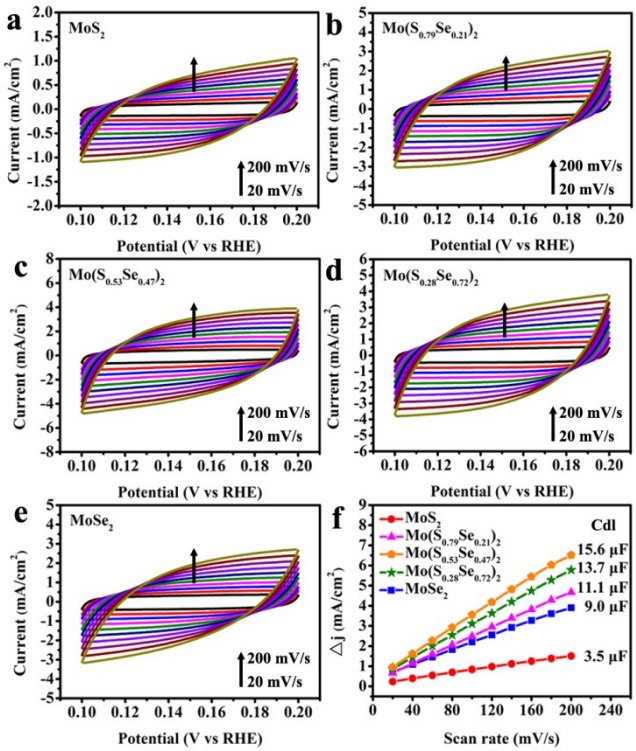

Fig. S6 Cyclic voltammetry curves of vertically oriented 3D $MoS_{2(1-x)}Se_{2x}$ alloy nanosheets in the potential region of 0.1-0.2 V *vs* RHE at different scan rate (20, 40, 60 mV s^{-1}, *etc.*), (b) The current density variation Δj at 0.15 V *vs* RHE plotted against scan rate linearly fitted to acquire C_{dl}.

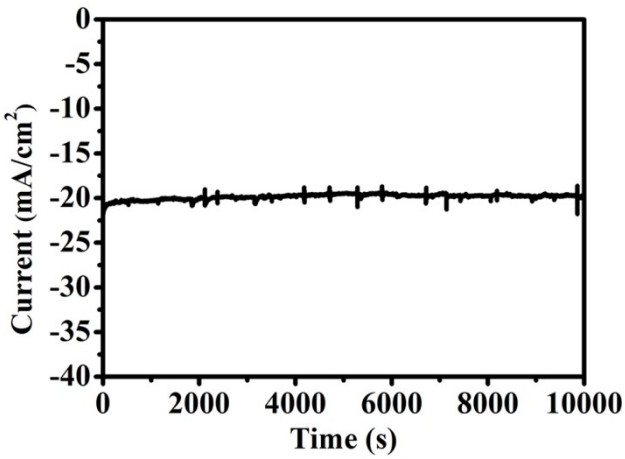

Fig. S7 Chronoamperometric curve of vertically oriented 3D $Mo(S_{0.53}Se_{0.47})_2$ nanosheets on carbon cloth under a constant overpotential of 200 mV for 10000s.

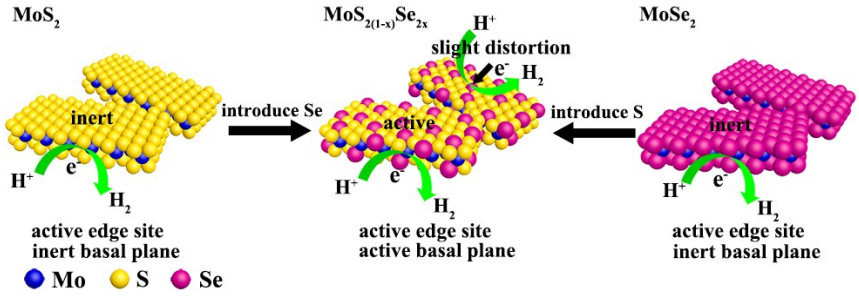

Fig. S8 Schematic illustration of HER electrocatalytic activity for vertically oriented 3D $MoS_{2(1-x)}Se_{2x}$ nanosheets.

Table S1 Comparison of previous reported MoS_2 and $MoSe_2$ based HER electrocatalysts and our electrocatalyst.

Catalyst	Morphology	Oneset potential η_0 (mV)	η_{10} (mV)	Tafel slope (mV dec^{-1})	Ref.
$MoS_{2(1-x)}Se_{2x}$	vertical nanosheet	121	183	55.5	Present work
2H MoS_2	nanosheet	250	-	75-86	S6
1T MoS_2		100	-	40	
2H MoS_2	nanosheet	200	320	117	2
1T MoS_2		135	187	43	
MoS_2	nanosheet	155	195	50	8
MoS_2	porous film	-	-	41-45	S7
MoS_2	nanosheet	-	-	140-145	S8
MoS_2	vertical film	200	-	86	S9
$MoSe_2$	vertical film	200	-	105	
$MoSe_2$	vertical	-	250	59.8	18

	nanofilm				
$MoSe_2$	macroporous film	150	250	80	S10
$MoSe_{2-x}$	nanosheet	170	288	98	S11
$MoSe_2$	nanosheet	70	182	69	S12
$MoS_{2(1-x)}Se_{2x}$	monolayer	-	273	100	10
MoS_2		-	381	99	
$MoSe_2$	nanosheet	-	348	68	S13
$Mo(S_xSe_{1-x})_2$		-	271	57	
MoS_2		-	219	91	
$MoSe_2$	nanoflake	-	181	45	12
$MoS_{2(1-x)}Se_{2x}$		-	164	48	
MoO_3/MoS_2	core-shell nanowire	150	-	50	S14
MoS_2/MoO_2	porous nanosheet	104	-	76.1	S15
MoS_2/MoO_2	3D heterostructure	142	-	35.6	S16

MoS_2/rGO/PPD/O-MWCNT	3D network	90	-	48	3
MoO_2@N-doped MoS_2	nanosheet	156	-	47.5	S17

References

S1 G. Kresse and J. Furthmuller, *Comput. Mater. Sci.*, 1996, **6**, 15.

S2 G. Kresse and D. Joubert, *Phys. Rev. B*, 1999, **59**, 1758.

S3 J. D. Pack and H. J. Monkhorst, *Phys. Rev. B*, 1977, **16**, 1748.

S4 D. Voiry, H. Yamaguchi, J. Li, R. Silva, D. C. B. Alves, T. Fujita, M. Chen, T. Asefa, V. B. Shenoy, G. Eda and M. Chhowalla, *Nat. Mater.*, 2013, **12**, 850.

S5 C. G. Van de Walle and J. Neugebauer, *J. Appl. Phys.*, 2004, **95**, 3851.

S6 D. Voiry, M. Salehi, R. Silva, T. Fujita, M. Chen, T. Asefa, V. B. Shenoy, G. Eda and M. Chhowalla, *Nano Lett.*, 2013, **13**, 6222.

S7 Z. Lu, H. Zhang, W. Zhu, X. Yu, Y. Kuang, Z. Chang, X. Lei and X. Sun, *Chem. Commun.*, 2013, **49**, 7516.

S8 Y. Yu, S.-Y. Huang, Y. Li, S. N. Steinmann, W. Yang and L. Cao, *Nano Lett.*, 2014, **14**, 553.

S9 D. Kong, H. Wang, J. J. Cha, M. Pasta, K. J. Koski, J. Yao and Y. Cui, *Nano Lett.*, 2013, **13**, 1341.

S10 F. H. Saadi, A. I. Carim, J. M. Velazquez, J. H. Baricuatro, C. C. L. McCrory, M. P. Soriaga and N. S. Lewis, *ACS Catal.*, 2014, **4**, 2866.

S11 X. Zhou, J. Jiang, T. Ding, J. Zhang, B. Pan, J. Zuo and Q. Yang, *Nanoscale*, 2014, **6**, 11046.

S12 B. Qu, X. Yu, Y. Chen, C. Zhu, C. Li, Z. Yin and X. Zhang, *ACS Appl. Mater. Interfaces*, 2015, **7**, 14170.

S13 B. Xia, L. An, D. Gao, S. Shi, P. Xi and D. Xue, *Crystengcomm*, 2015, **17**, 6420.

S14 Z. B. Chen, D. Cummins, B. N. Reinecke, E. Clark, M. K. Sunkara and T. F. Jaramillo, *Nano. Lett.*, 2011, **11**, 4168.

S15 L. J. Yang, W. J. Zhou, D. M. Hou, K. Zhou, G. Q. Li, Z. H. Tang, L. G. Li and S. W. Chen, *Nanoscale*, 2015, **7**, 5203.

S16 R. D. Nikam, A. Y. Lu, P. A. Sonawane, U. R. Kumar, K. C. Yadav, L. J. Li and Y. T. Chen, *ACS Appl. Mater. Interfaces*, 2015, **7**, 23328.

S17 W. J. Zhou, D. M. Hou, Y. H. Sang, S. H. Yao, J. Zhou, G. Q. Li, L. G. Li, H. Liu and S. W. Chen, *J. Mater. Chem. A*, 2014, **2**, 11358.